THE JOURNAL OF BIOLOGICAL CHEMISTRY
Vol. 272, No. 2, Issue of January 10, pp. 1117–1126, 1997

Printed in U.S.A.

Loss of Binding and Entry of Liposome-DNA Complexes Decreases Transfection Efficiency in Differentiated Airway Epithelial Cells*

(Received for publication, May 28, 1996, and in revised form, October 15, 1996)

Hirotoshi Matsui‡, Larry G. Johnson, Scott H. Randell, and Richard C. Boucher

From the Cystic Fibrosis/Pulmonary Research and Treatment Center, University of North Carolina, Chapel Hill, North Carolina 27599-7248

The target cells for gene therapy of cystic fibrosis lung disease are the well differentiated cells that line airway lumens. Employing cultures of airway epithelial cells that grow like "islands" and exhibit a continuum of cellular differentiation, we studied the mechanisms that render well differentiated cells more difficult to transfect with cationic liposomes than poorly differentiated cells. The poorly differentiated cells at the edge of the islands were transfectable with liposome-DNA complexes (pCMVβ:LipofectACE = 1:5 (w/w)), whereas the more differentiated cells in the center of the islands were not. Evaluation of the steps leading to lipid-mediated transfection revealed that edge cells bound more liposome-DNA complexes, in part due to a more negative surface charge (as measured by cationized ferritin binding), and that edge cells internalized more liposome-DNA complexes than central cells. Edge cells exhibited receptor-mediated endocytosis of LDL, pinocytosis of 10-nm microspheres, and phagocytosis of 2-μm microspheres, whereas central cells were only capable of receptor-mediated endocytosis. Cytochalasin B, which inhibited pinocytosis by 65% and phagocytosis by 93%, decreased edge cell liposome-DNA complex entry by 50%. Potassium depletion, which decreased phagocytosis by >90% but had no effect on pinocytosis, inhibited edge cell liposome-DNA complex entry by 71%. These results indicate that liposome-DNA complexes enter edge cells via phagocytosis and that this pathway is not detectable in central cells. In conclusion, both reduced negative surface charge and absence of phagocytosis internalization pathways in relatively differentiated cells may explain differentiation-dependent decrements in cationic liposome-mediated gene transfer in airway epithelia.

Inefficiency of gene transfer is one of the major problems confronting cationic liposomes as vectors for cystic fibrosis (CF)[1] gene therapy. For successful gene therapy of CF lung disease, the cystic fibrosis transmembrane conductance regulator (CFTR) cDNA must be expressed in the well differentiated epithelial cells lining the airways of CF patients. Although cationic liposomes deliver genes efficiently into some cell lines and primary culture cells of certain tissues (1–6), the transfection efficiency in well differentiated airway cells *in vivo* is limited (7), paralleling observations with adenoviral vectors (8–10). Studies designed to identify rate-limiting factors for lipid-mediated gene transfer in undifferentiated cell lines revealed that nontransfectable cells internalized liposome-DNA complexes as well as transfectable cells, suggesting that entry across the nuclear membrane rather than across the plasma membrane is the rate-limiting factor in poorly transducible undifferentiated cells (11). Studies have not been performed to identify the rate-limiting steps in well differentiated *versus* poorly differentiated cells of the same cell type.

To identify the mechanisms that may account for differentiation-dependent differences in the efficiency of lipid-mediated gene transfer in airway epithelial cells, we used *in vitro* cell culture systems that simultaneously contain populations of both differentiated and dedifferentiated airway cells. When human or rat airway epithelial cells are cultured on collagen-coated membranes with defined media, dedifferentiated cells proliferate and redifferentiate into ciliated cells and goblet cells (12, 13). At a point in between these two stages (dedifferentiated and redifferentiated), *e.g.* day 5, airway epithelial cells grow as "islands" or flat colonies. The "edge cells" of these "cellular islands" show features of wound repairing or poorly differentiated cells with lamellipodia (10), whereas the cells in the center are surrounded by tight junctions and have several morphological features of differentiation at the apical membrane, including glycocalyx expression and microvilli.

In this study, we first measured cationic lipid-mediated transduction in cellular islands derived from both human and rat airway epithelial cells. We subsequently focused on the rat system to identify cellular factors that may regulate the relatively efficient lipid-mediated gene delivery to poorly differentiated (edge) airway epithelial cells as compared with redifferentiated (central) airway epithelial cells.

MATERIALS AND METHODS

Human Bronchial Cell Isolation and Culture

Human bronchial epithelial cells were cultured using procedures similar to those described by Gray *et al.* (13) with the following modifications. Portions of main stem or lobar bronchi representing excess donor tissue were obtained at the time of lung transplantation under the auspices of the UNC Institutional Committee on the Protection of the Rights of Human Subjects. Epithelial cells were removed from the specimens by protease type 14 (Sigma) digestion as described (14) but omitting the filtration step. Cells were plated at a density of 2.5×10^5 cells/24-mm Transwell-Col® insert (Costar Co., Cambridge, MA; diameter, 24.5 mm; pore size, 0.4 μm) in modified LHC9 medium (15). The modifications included using a 50:50 mixture of LHC Basal (Biofluids, Rockville, MD) and Dulbecco's modified Eagle's medium with high glucose as the base, reducing the epidermal growth factor concentration to 0.5 ng/ml, adjusting the retinoic acid concentration to 5×10^{-8} M, and supplementation with 0.5 mg/ml bovine serum albumin and 0.8% bo-

* This work was supported by National Institutes of Health Grant HL51818 and Cystic Fibrosis Foundation Grant S880. The costs of publication of this article were defrayed in part by the payment of page charges. This article must therefore be hereby marked "*advertisement*" in accordance with 18 U.S.C. Section 1734 solely to indicate this fact.

‡ To whom correspondence should be addressed: 7129 Thurston-Bowles Bldg., CB 7248, University of North Carolina, Chapel Hill, NC, 27599-7248. Tel.: 919-966-7044; Fax: 919-966-7524; E-mail: comodo@med.unc.edu.

[1] The abbreviations used are: CF, cystic fibrosis; RTE, rat tracheal epithelial; CFTR, cystic fibrosis transmembrane conductance regulator; DIC, differential interference contrast; LDL, low density lipoprotein; PBS, phosphate-buffered saline; X-gal, 5-bromo-4-chloro-3-indolyl β-D-galactoside; BrdUrd, 5-bromo-2′-deoxyuridine.

vine pituitary extract. Under these conditions, the seeded cells initially formed small "islands." Day 5 cultures were used for transfection with liposome-DNA complexes (see below).

Rat Tracheal Epithelial (RTE) Cell Isolation and Culture

RTE cells were isolated and cultured based on the methods of Kaartinen *et al.* (12). Briefly, male Fisher 344 rats (200–225 g) (Charles River, Southbridge, MA) were euthanized with CO_2 asphyxiation. Tracheas were cannulated, excised, and filled with a 1% solution of protease type 14 in Ham's F12 medium and incubated for 24 h at 4 °C. Epithelial cells were removed from the trachea by flushing with media, counted, and plated onto the apical surface of Transwell-Col® tissue culture inserts at a density of 1.2×10^5 cells/well. The culture medium was Dulbecco's modified Eagle's medium/F12 medium supplemented with insulin (10 μg/ml), hydrocortisone (0.1 μg/ml), cholera toxin (0.1 μg/ml), transferrin (5 μg/ml), phosphoethanolamine (50 μM), ethanolamine (80 μM), epidermal growth factor (25 ng/ml), bovine pituitary extract (1%), retinoic acid (5×10^{-8} M), penicillin-streptomycin (50 units/ml, 50 μg/ml) and bovine serum albumin (3 mg/ml). Experiments were performed on the fifth day of culture, when 50–70% of the membrane was covered by cells.

Morphology of Cultured RTE Cells

Electron Microscopy—Day 5 RTE cells were fixed with 2% paraformaldehyde and 2% glutaraldehyde in PBS for 1 h, incubated with osmium tetroxide (OsO_4), and embedded in Epon. Sections (90 nm) were cut with an LKB Huxley ultramicrotome, placed on copper grids, and examined by transmission electron microscopy (Zeiss 900). Photographs taken serially were digitized with a flatbed scanner (ScanJet4C, Hewlett Packard), integrated, and printed to illustrate two cells in a single picture after brightness and contrast were adjusted.

Staining of Actin Filaments—Filamentous actin (F-actin) of day 5 RTE cells was stained with tetramethylrhodamine-labeled phalloidin (Sigma) (16). RTE cells were fixed, permeabilized, and stained with a solution of 4% paraformaldehyde, 0.2% Triton X, and 0.5 μg/ml tetramethylrhodaminyl phalloidin for 20 min at room temperature.

DNA

pCMVβ (Clontech, Palo Alto, CA) was amplified in DH5F-α and purified on a CsCl gradient. The pCMVCFTR plasmid was constructed by restriction enzyme digestion of pCMVβ with *Not*I followed by ligation of the CFTR cDNA fragment from pVL-CFTR (a gift from Elmer Price, University of Missouri) into the *Not*I restriction site.

Labeling of Liposomes

LipofectACE® (Life Technologies, Inc.), a 1:2.5 (w/w) formulation of dimethyldioctadecylammonium bromide and dioleoylphosphatidylethanolamine, was labeled with CM-DiI (Molecular Probes, Eugene, OR) based on modification of the method of Claassen (17). Briefly, 200 μg of LipofectACE® was incubated with 1 μg of CM-DiI (1 mg/ml in ethanol) for 30–60 min at room temperature, followed by mixing with same volume of lymphocyte separation medium (Boehringer Mannheim) and centrifugation at 14,000 rpm for 10 min. The supernatant containing CM-DiI-labeled liposomes was utilized for the studies within 12 h. To confirm that free dye was precipitated and removed by centrifugation, the same concentration of CM-DiI solution was centrifuged in the absence of liposomes. The supernatant was added to RTE cultures and incubated as described under "Measurement of Binding and Entry," and no signal was detected by fluorescence microscopy.

Double Labeling of Liposome-DNA Complexes in a Cell-free System

CM-DiI (0.1 mg/ml in ethanol) was added to LipofectACE® solution at a final concentration of 0.2 μg/ml, and the mixture was incubated at room temperature for 1 h. When viewed at high concentrations, free CM-DiI formed clumps that resembled labeled liposomes by fluorescence microscopy. We carefully determined the concentration (0.2 μg/ml) at which the liposomes became labeled, but the dye did not form detectable clumps. We confirmed that clumps were not formed at this concentration by fluorescence microscopy (DMIRB, Leica, Wetzlar, Germany) with × 1000 magnification (× 100 objective and × 10 ocular). No particulate fluorescence was detected in the absence of liposomes at the concentration (0.2 μg/ml) of CM-DiI used in this study. pCMVCFTR (0.1 mg/ml) was labeled with BOBO-1 (Molecular Probes). BOBO-1 is a dimeric cyanine acid stain that intercalates into DNA bases by binding noncovalently. After incubation for 1 h in a solution of 5 μM BOBO-1 at room temperature, the labeled DNA (5 μg) was vigorously mixed with the CM-DiI-labeled liposomes (25 μg) and was incubated for 30 min at room temperature to obtain double labeling of liposome-DNA complexes. After dilution with 400 μl of the culture medium containing 0.2 μg/ml of CM-DiI and 5 μM of BOBO-1, the labeled complexes were observed under a fluorescent microscope with a × 100 objective. Due to the broad excitation and emission spectrum of CM-DiI, we used a GFP (green fluorescent protein) filter set (Chroma, Brattleboro, VT) to visualize BOBO-1 separately from CM-DiI.

Delivery of Liposome-DNA Complexes

Reporter Gene Assay—The pCMVβ plasmid and unlabeled LipofectACE® were mixed in a ratio of 1:5 (w/w), followed by incubation for 15–30 min at room temperature before dilution with culture media. A single well of day 5 RTE cells or human bronchial epithelial cells was transfected with the mixture of 5 μg of DNA and 25 μg of liposomes diluted with 500 μl of the culture medium on the apical surface. The basolateral surface of the insert was bathed in 2 ml of culture medium only. Transfection was performed for 3 h at 37 °C. After the liposomes were removed by gentle washing, cells were maintained in the culture medium for 48 h at 37 °C and stained with 5-bromo-4-chloro-3-indolyl β-D-galactoside (X-gal) (see below).

Measurement of Binding and Entry—To measure binding, 5 μg of pCMVCFTR complexed to 25 μg of labeled liposomes was incubated with cells at 4 °C for 3 h or at 37 °C in the presence of a metabolic inhibitor, antimycin A (Sigma) (1 μg/ml, 30 min preincubation prior to dosing). The sum of binding and entry of liposome-DNA complexes was measured by incubating the labeled complexes with the RTE cells at 37 °C for 3 h. RTE cells were then washed twice with PBS, fixed with 4% paraformaldehyde, and examined by fluorescence microscopy.

X-Gal Staining

48 h after transfection, the cells were stained with X-gal (Sigma) solution as described previously (18). Briefly, cells on collagen-coated membranes were fixed with 0.5% glutaraldehyde for 10 min, washed twice with PBS containing 1 mM $MgCl_2$, and stained with 1 mg/ml X-gal in a solution of 1 mM $MgCl_2$, 5 mM $K_3Fe(CN)_6$, 5 mM $K_4Fe(CN)_6$ for 4 h.

Localization of Proliferating Cells

To measure cell proliferation, cells were labeled with 5-bromo-2′-deoxyuridine (BrdUrd) using a commercially available kit (Boehringer Mannheim). On day 5, RTE cells were incubated with culture medium containing 10 μmol/liter of BrdUrd for 1 h at 37 °C. The cells were then fixed with 70% ethanol in 50 mM glycine buffer (pH 2.0) for 20 min at −20 °C, washed with PBS, and incubated with mouse monoclonal anti-BrdUrd antibody for 30 min at 37 °C and then with fluorescein-conjugated anti-mouse IgG for 30 min at 37 °C.

Measurement of Cationized Ferritin Binding

Day 5 RTE cells were incubated for 1 h at 4 °C with 50 μg/ml of fluorescein-labeled cationized ferritin (Molecular Probes) (19–21) in 500 μl of the culture medium on the apical surface and with unmodified culture medium on the basolateral surface. After washing twice with PBS and fixation in 4% paraformaldehyde, the cells were photographed or reserved for measurement of fluorescence intensity as described below.

Measurement of Endocytic Activity

10-nm and 2-μm fluorescent latex microspheres (carboxylate-modified) were purchased from Molecular Probes to estimate rates of pinocytosis and phagocytosis, respectively (22). DiI-labeled low density lipoprotein (DiI-LDL) was also obtained from Molecular Probes as a marker of receptor-mediated endocytosis (23). These markers were diluted in 500 μl of culture medium at a final concentration of 0.006% for the 10-nm and 2-μm particles and 10 μg/ml for DiI-LDL. These were individually applied to the apical surface of RTE cells and incubated for 3 h at 37 °C with 2 ml of culture medium alone on the basolateral surface. After washing twice with PBS, the fluorescence intensity was measured as described below.

Inhibition of Endocytosis by Cytochalasin B

RTE cells were preincubated for 30 min in culture medium containing 5 μg/ml of cytochalasin B (Sigma), which blocks phagocytosis and pinocytosis but not receptor-mediated endocytosis (22, 24) by inhibiting actin polymerization. The cells were then incubated with labeled liposome-DNA complexes and specific endocytic markers in the presence of the same concentration of cytochalasin B for 3 h at 37 °C. The fluorescence intensity of each marker was then measured in edge cells after washing twice with PBS.

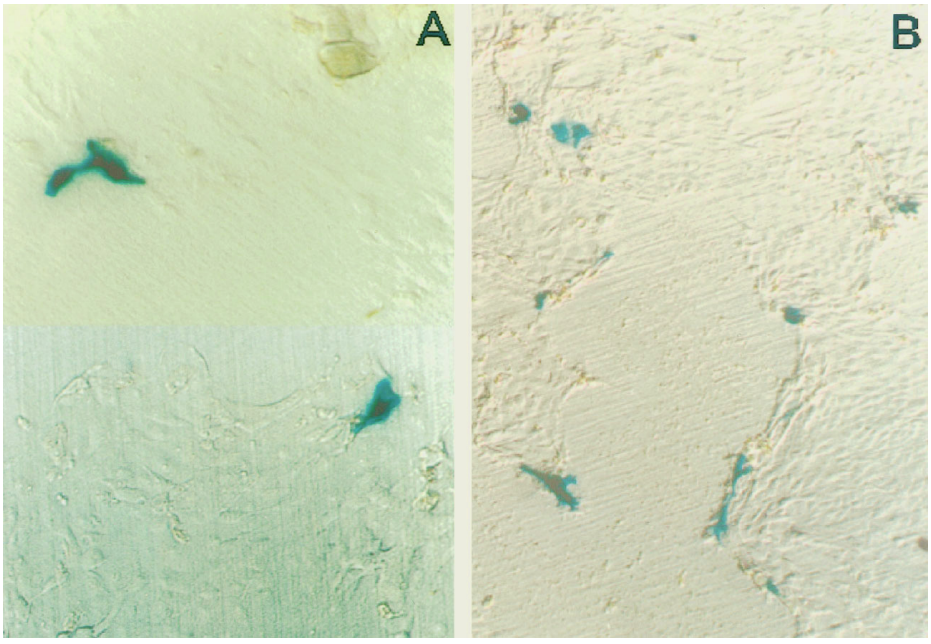

FIG. 1. **Pattern of gene transfer in cell islands.** Human (*A*) and rat (*B*) airway epithelial cells proliferated and spread like islands on collagen-coated membranes. These cells were incubated with liposome-DNA complexes (25 μg of LipofectACE® and 5 μg of pCMVβ plasmid) for 3 h and stained with X-gal 48 h later. A few LacZ-expressing blue cells were detected predominantly on the edge of "cellular islands."

Effect of Potassium (K^+) Depletion on Endocytic Activity

RTE cells were treated according to the method of Larkin *et al.* (25). Briefly, cultures were washed twice with K^+-free buffer (140 mM NaCl, 20 mM HEPES, pH 7.4, 1 mM $CaCl_2$, 1 mM $MgCl_2$) and incubated in hypotonic buffer (K^+-free buffer diluted 1:1 with distilled water) for 5 min at 37 °C. The cells were then washed twice and incubated with K^+-free buffer for 15 min at 37 °C. The pretreated cells were then incubated with pinocytic and phagocytic markers (10-nm and 2-μm microspheres, respectively) or liposome-DNA complexes in K^+-free buffer for 1 h at 37 °C. Postincubation, RTE cells were washed twice with PBS, and the fluorescence intensity of edge cells was quantified. In this experiment, the incubation time was decreased to 1 h, because a 3-h incubation in this buffer induced cell detachment from the collagen-coated membranes. Control cells for this experiment were treated identically except that 4 mM KCl was added to the K^+-free buffer.

Measurement of Fluorescence Intensity

The RTE cells were examined under fluorescent microscopy (DMIRB, Leica) with a × 20 (0.40 numerical aperture) objective after incubation with CM-DiI-labeled liposome-DNA complexes with cationized ferritin or with specific endocytic markers. Digital images (740 × 570 pixels) were acquired with a cooled CCD camera (Hamamatsu C5985, Hamamatsu, Japan) and were analyzed with an image processing system (MetaMorph, Universal Imaging Co., West Chester, PA). Exposure time and camera gain were constant for each experiment. Five areas were selected from each sample to obtain a fluorescent image, a background image, and a differential interference contrast (DIC) image of each area. Background images were acquired by defocusing the corresponding fluorescent images (maximally out of focus) and were subtracted from them. From the DIC images, inner and outer borders of edge cells were traced manually, and these borders were transferred to the corresponding background-subtracted fluorescent images. The fluorescence intensity over the edge cell area was integrated and normalized to the area. Central cells were similarly traced, and fluorescence intensity was determined. Care was taken to leave a narrow zone inside the edge cell boundary to avoid cross-contamination of the signals.

Statistics

Unless otherwise stated, data are displayed as mean ± S.D. ($n = 5$). $p < 0.05$ is considered as significant using a paired t test for the comparison of edge *versus* central cells or Student's t test for other comparisons.

RESULTS

Distribution of LacZ-expressing Airway Epithelial Cells

Day 5 human bronchial epithelial cells and RTE cells were transfected with pCMVβ-LipofectACE® (1:5, w/w) complexes, and 48 h later they were stained with X-gal. As shown in Fig. 1, LacZ-expressing blue cells were selectively located in the periphery of the cellular islands both in the rat and human airway epithelial cultures. The 48-h time lag between gene delivery and staining occasionally made it difficult to identify the origin of the blue cells detected; *i.e.* rare central blue cells might have been located on the edge when incubated with liposome-DNA complexes. Therefore, we defined the edge area as "edge cells" plus the single layer of cells adjacent to "edge cells" only for this section. Using this criterion, the transfection rate in RTE cells was low even in the edge area (4.0% ± 1.1% (mean ± S.D.), $n = 4$), whereas the central cells were rarely transfected (0.2 ± 0.2% (mean ± S.D.), $n = 4$). The transfection rate was calculated as the blue area divided by the total edge or central area.

Morphology of RTE Cells

Electron Micrograph—Day 5 RTE cells cultured on collagen substrates were examined under transmission electron microscopy (Fig. 2*A*). Electron microscopy revealed that day 5 RTE cells were generally flat or squamous in appearance. The central cells frequently exhibited microvilli on the apical surface and were encircled with tight junctions. They also occasionally exhibited a few cilia and glycocalyx. In contrast, edge cells were flatter with little glycocalyx or microvilli, and generally had a relatively smooth surface without apparent polarization.

F-actin Staining—Fig. 2, *B* and *C*, shows that edge cells extend filopodia and lamellipodia filled with actin filaments at their leading edge. Lamellipodia are involved in cell movement and phagocytosis (16). In contrast, central cells exhibited F-actin along lateral plasma membrane. These perijunctional actin filaments are necessary for the epithelial barrier integrity (26, 27), consistent with formation of polarized epithelia.

Localization of Proliferating Cells

To examine the relationship between cell proliferation and transfection efficiency, BrdUrd uptake was determined in day 5 RTE cells. Fig. 3 shows that the distribution of BrdUrd-labeled cells differed from that of LacZ-expressing cells. Distribution of BrdUrd-positive cells was patchy, not continuous along the rim of the islands. This result suggests that edge cells are not proliferating more frequently than central cells. Hence,

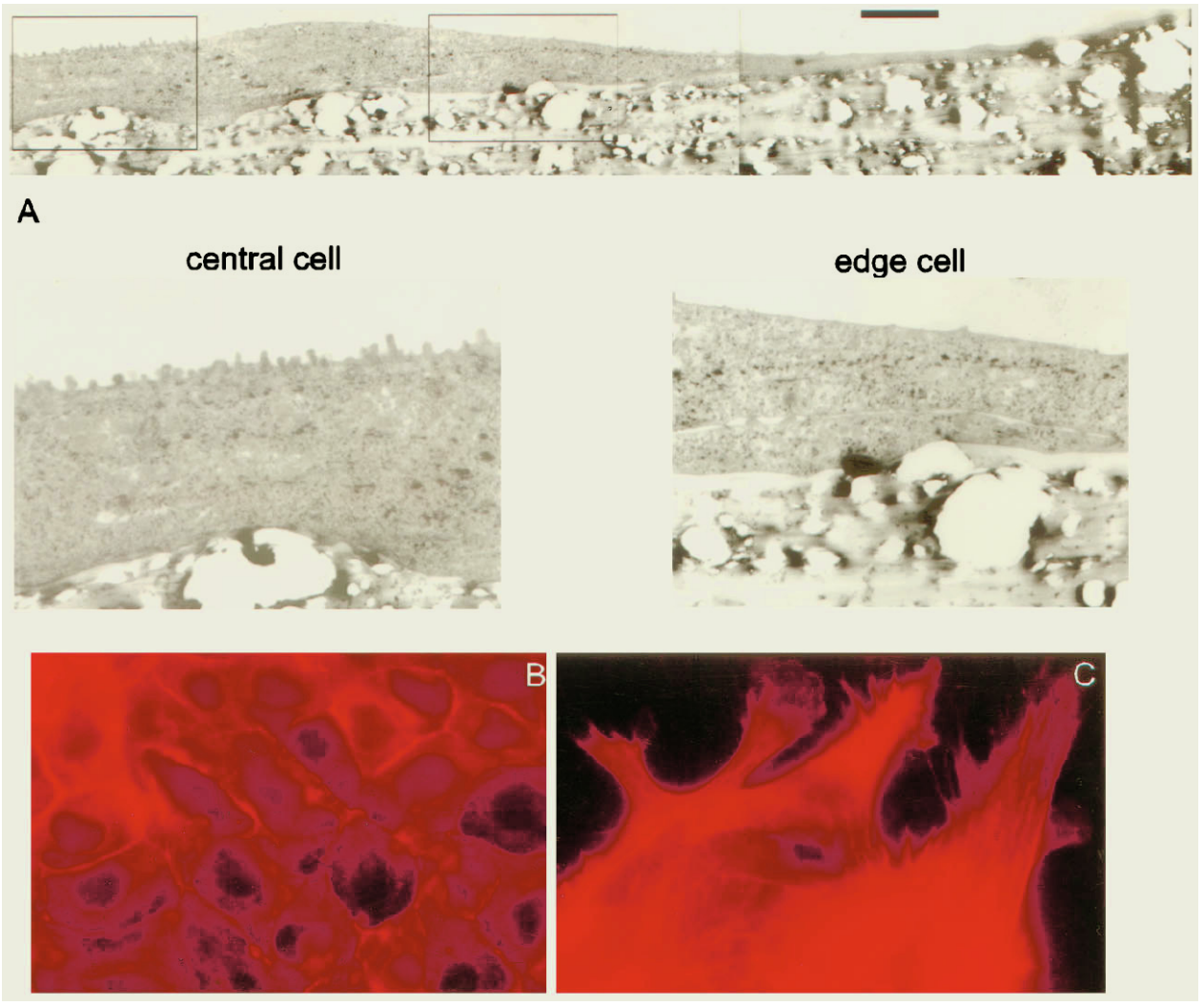

FIG. 2. **Morphology of RTE cell "islands."** *A*, this composite electron micrograph of day 5 RTE cells is derived from three continuous pictures. The poorly infiltrated Transwell-Col® membrane is below the cells. The *two rectangular highlighted areas* were enlarged to show the details of a central cell (*left*) and an edge cell (*right*). Central cells frequently exhibited signs of differentiation and polarization including microvilli, glycocalyx, and occasional cilia. In contrast, flatter edge cells had a relatively smooth surface with few microvilli and little glycocalyx. *Bar*, 5 μm. *B* and *C*, RTE cells were stained with fluorescently labeled phalloidin to detect actin filaments. Central cells (*B*) exhibit F-actin distributed along the lateral plasma membrane, consistent with polarized epithelia. Edge cells (*C*) extend lamellipodia and filopodia filled with actin filaments, showing a feature of poorly differentiated regenerating cells.

proliferation is not likely to be a major reason for more efficient transfection of edge cells.

Efficiency of Liposome Incorporation into Liposome-DNA Complexes

Liposome-DNA complexes were double labeled in a cell-free system to test whether all the liposomes were incorporated into liposome-DNA complexes at the ratio of DNA to lipid used in this mixture (1:5, w/w). CM-DiI labeling (Fig. 4*A*) and BOBO-1-labeling (Fig. 4*B*) show that more than 90% of the CM-DiI-labeled particles were co-localized with BOBO-1-labeled particles. Based on these data, we assume that the majority of CM-DiI labeling in the following experiments represents liposome-DNA complexes.

Binding and Entry of Labeled Liposome-DNA Complexes

CM-DiI-labeled liposome-DNA complexes were incubated with RTE cells for 3 h at 4 and 37 °C to examine binding and entry of the complexes, respectively. The labeled complexes were predominantly detected on the edge cells at both 4 (Fig. 5*A*) and 37 °C (Fig. 5*B*), which indicates that both binding and internalization of the liposome-DNA complexes occur selectively in the edge cells. To quantitate the magnitude of binding and internalization for each type, the fluorescence intensity of cell-associated liposome-DNA complexes at 4 °C was measured and compared with the fluorescence intensity at 37 °C. Fluorescent signals in the edge cells at 37 °C were almost 3-fold greater than at 4 °C (Fig. 5*C*), with 35% of the total signal derived from binding and 65% from internalization. There was no significant difference between cell-associated fluorescence intensity detected at 4 °C and that detected at 37 °C in the presence of the metabolic inhibitor antimycin A (fluorescence intensity measured as gray level/pixel was 45.5 ± 8.2 at 4 °C and 32.1 ± 11.5 at 37 °C with antimycin A (mean ± S.D.), n = 5). This result indicates that binding efficiency at 4 °C is similar to that at 37 °C. No temperature-dependent difference in fluorescence intensity was detected in central cells.

Measurement of Cationized Ferritin Binding

To determine whether increased binding of cationic liposome-DNA complexes by edge cells reflected a more negative cell surface charge, we incubated RTE cells with cationized

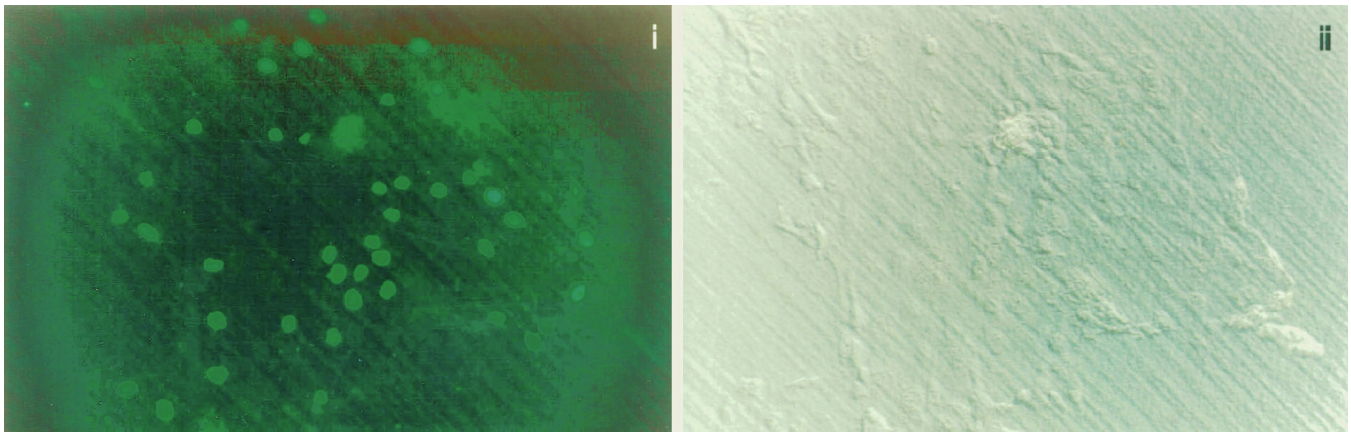

FIG. 3. **Cellular proliferation, as indexed by BrdUrd uptake, in RTE cells.** The distribution of proliferating cells were examined by BrdUrd uptake. BrdUrd-positive cells exhibited a patchy distribution in cellular islands. The distribution of the LacZ-expressing cells was different from the distribution of the cells incorporating BrdUrd (see Fig. 1). *i*, fluorescent image; *ii*, DIC image.

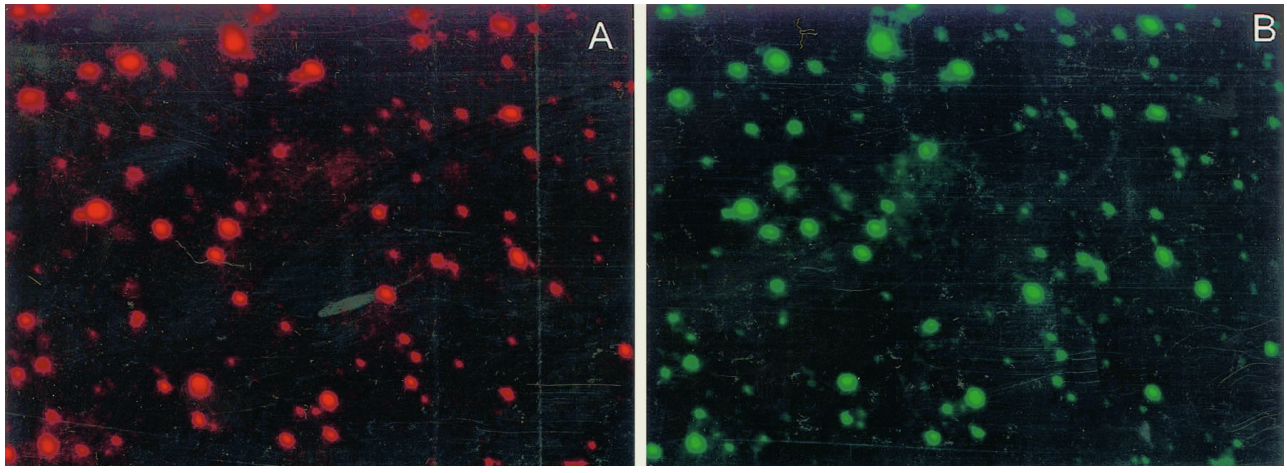

FIG. 4. **Fluorescent double labeling of liposome-DNA complexes.** Liposome-DNA complexes (25 μg of liposome and 5 μg of plasmid in 500 μl of culture media) were labeled with CM-DiI (liposome stain, *red*; *panel A*) and BOBO-1 (DNA stain, *green*; *panel B*) and observed with a 100 $\times$ objective. In a 1:5 (w/w) mixture of DNA and liposomes, more than 90% of the particles showed colocalization of the two dyes.

ferritin at 4 °C and compared edge and central cell binding. Fig. 6*A* shows that edge cells bound more cationized ferritin, suggesting a more negative surface charge than central cells. Quantitation of the fluorescent signal demonstrated that cationized ferritin binding was detected predominantly on the edge cells, whereas it was barely detectable on the central cells (9% of that measured on edge cells) (Fig. 6*B*).

Measurement of Endocytic Activity

To determine the endocytic capacity of edge and central cells, 10-nm latex microspheres (a marker of pinocytosis), 2-μm latex microspheres (a marker of phagocytosis), or DiI-LDLs (a marker of receptor-mediated endocytosis) were incubated with the cell islands for 3 h at 37 °C. Fig. 7, *A* and *B*, shows that only edge cells exhibited pinocytic and phagocytic activity. In contrast, both edge and central cells exhibited receptor-mediated endocytosis (Fig. 7*C*). Quantitatively, all of the markers showed significant peripheral distribution (Fig. 7*D*). Pinocytosis in the central cells was 6% of that detected in the edge cells, a value not significantly different from 0, and no phagocytosis was detectable in central cells. Only receptor-mediated endocytosis occurred to a significant degree in central cells (27% of that detected in edge cells). To confirm that LDL was internalized via receptor-mediated endocytosis, we tested whether LDL endocytosis was sensitive to K^+ depletion. Fluorescence intensity in central cells was significantly reduced by K^+ depletion (relative fluorescence intensity was 100% $\pm$ 11.3% in control, 63.4% $\pm$ 23.3% in K^+ depletion (mean $\pm$ S.D.), $n = 5$).

Inhibition of Endocytosis by Cytochalasin B

Each of the endocytic markers and labeled liposome-DNA complexes was incubated with RTE cells in the presence of 5 μg/ml of cytochalasin B. Fluorescence intensity was measured only in edge cells, because central cells did not exhibit phagocytosis or pinocytosis. Cytochalasin B inhibited phagocytosis and pinocytosis (93 and 65%, respectively), whereas receptor-mediated endocytosis was not reduced (Fig. 8). The entry of liposome-DNA complexes was partially blocked (50%), which suggests that actin polymerization was involved in the endocytic mechanism of the liposome-DNA complexes and that pinocytosis and/or phagocytosis was necessary for liposome-DNA entry.

Effects of Potassium Depletion on Endocytic Activity

Previous reports have indicated that phagosomes exhibit clathrin coats (28) and that an anti-clathrin antibody inhibits phagocytosis (29). Therefore, to distinguish between pinocytosis and phagocytosis as the entry route of liposome-DNA complexes, we tested the effects of K^+ depletion, which disassembles clathrin coats (25), thereby inhibiting phagocytosis. 10-nm

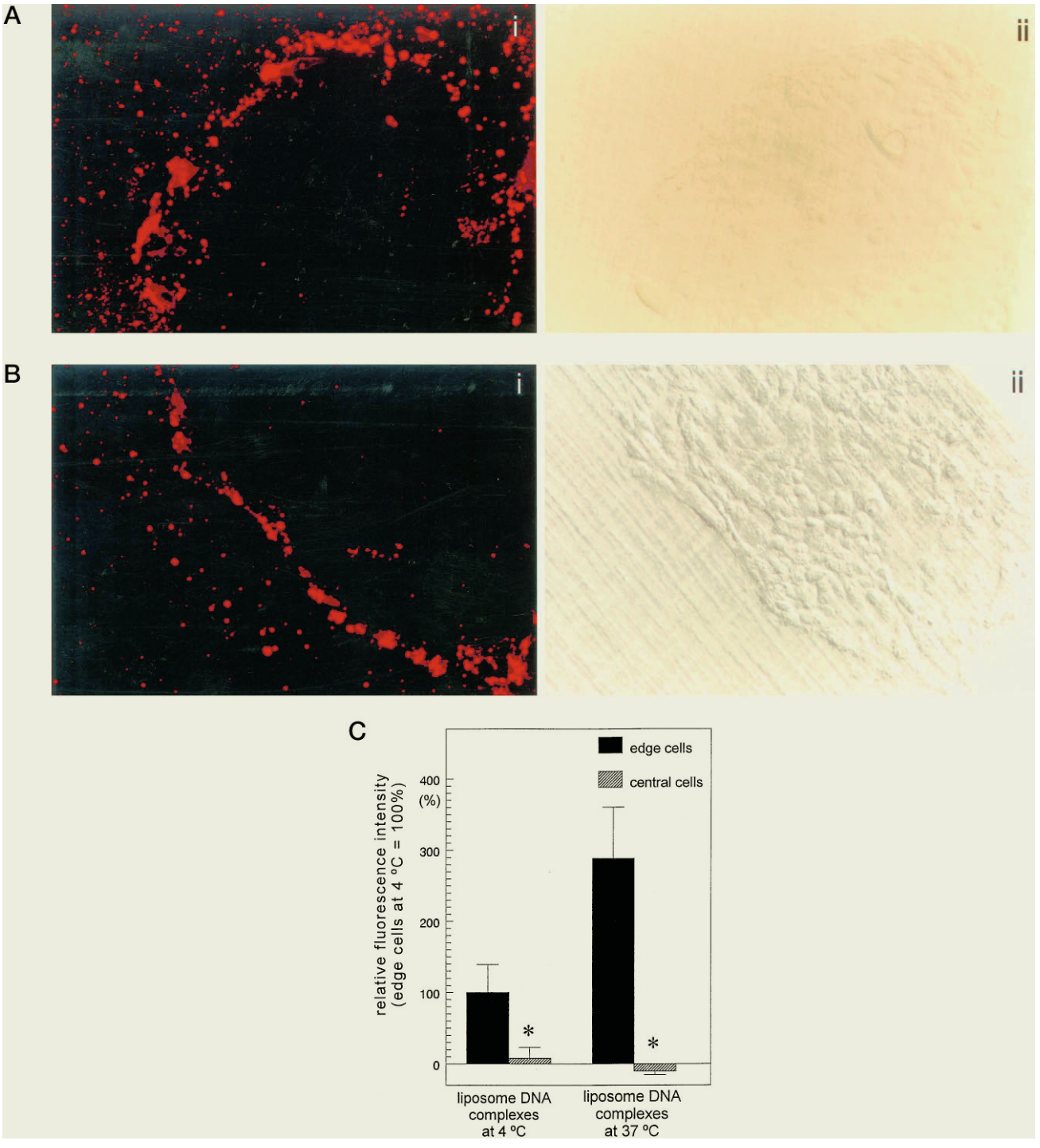

FIG. 5. **Distribution of labeled liposome-DNA complexes bound and endocytosed by cells in RTE islands at 4 °C and at 37 °C, respectively.** CM-DiI-labeled liposome-DNA complexes were incubated with day 5 RTE cells for 3 h at 4 and 37 °C. *A*, at 4 °C, labeled complexes were preferentially detected on edge cells. Background signals on collagen-coated membranes were higher than signals on central cells. *i*, fluorescent image; *ii*, DIC image. *B*, at 37 °C, a similar distribution pattern was seen, although the magnitude of the signals was greater. *i*, fluorescent image; *ii*, DIC image. *C*, quantitative data showed that both binding (signals at 4 °C) and entry ((signals at 37 °C) − (signals at 4 °C)) were predominantly detected in the edge cells. Fluorescence intensity is presented as a percentage relative to the fluorescence intensity of edge cells at 4 °C. Quantitative data are presented as mean ± S.D. ($n = 5$; *, $p < 0.05$).

and 2-μm microspheres were incubated with K^+-depleted RTE cells in K^+-free buffer. The fluorescence intensity of each probe was quantified only in the edge cells. Depletion of K^+ inhibited phagocytosis more than 90% but did not affect pinocytosis (Fig. 9*A*). Fig. 9*B* shows that liposome-DNA complex entry was blocked 71% by K^+ depletion, suggesting that phagocytosis is the primary entry pathway for liposome-DNA complexes.

DISCUSSION

Transfection efficiency must be increased before cationic liposomes become practical vectors for *in vivo* gene therapy of CF lung disease. Although some studies have reported successful transgene expression in airway epithelial cells *in vivo* (30–33), the levels of transduction are low, the distribution of transgene expression is patchy, and current clinical efficiency and safety

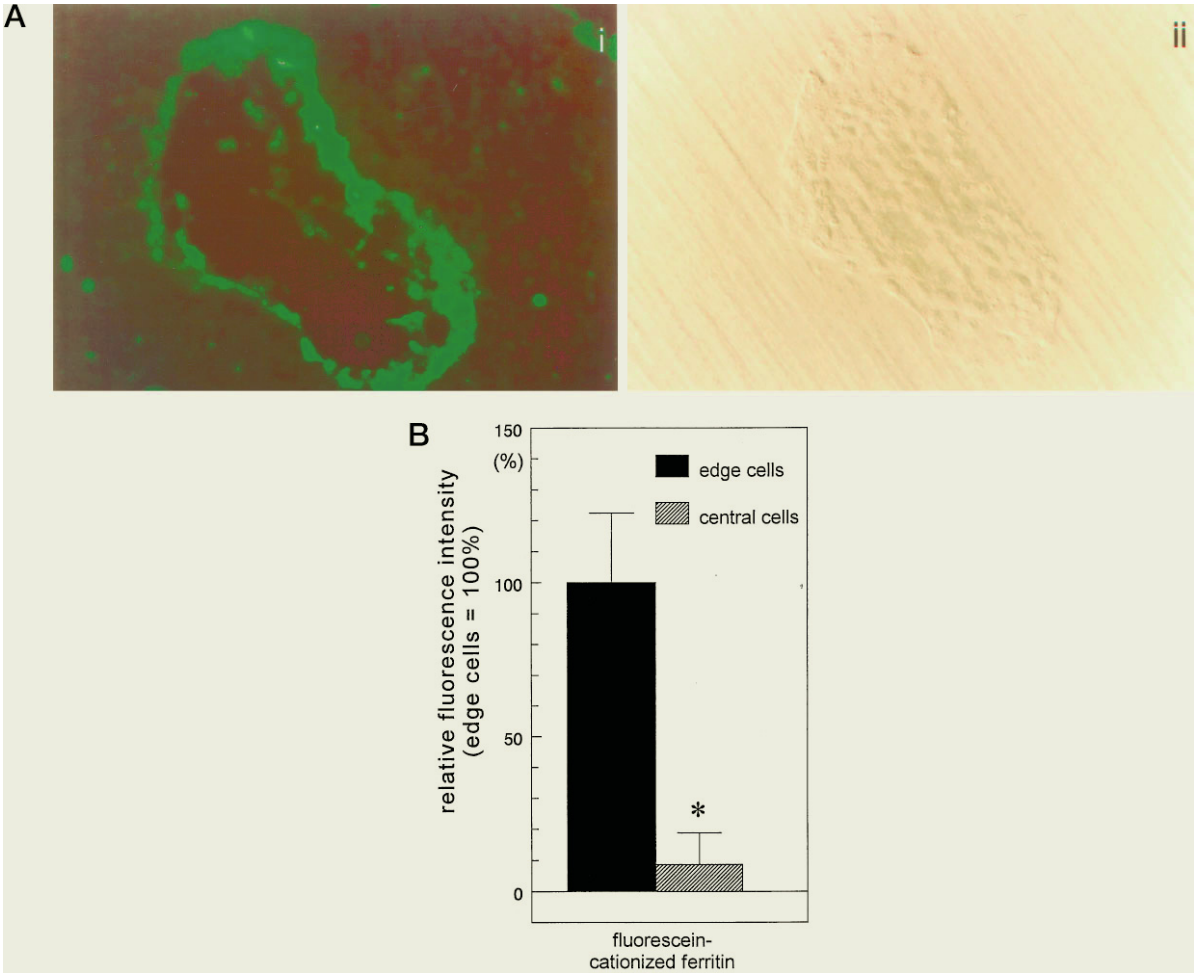

FIG. 6. **Comparison of surface negative charge of cells in RTE islands as measured with cationized ferritin attachment at 4 °C.** *A*, cationized ferritin was bound predominately by the edge cells after incubation with day 5 RTE cells for 1 h at 4 °C. *i*, fluorescent image; *ii*, DIC image. *B*, quantitative data confirmed that negative charge was detected in small amounts on the surface of the central cells, whereas edge cells bound 10 times more ferritin than central cells. Fluorescence intensity is presented as a percentage relative to the fluorescence intensity of the edge cells. Quantitative data are presented as mean ± S.D. ($n = 5$; *, $p < 0.05$).

studies report limited success (7). In an effort to improve the efficiency of gene transfer in airway epithelial cells, we investigated the cellular mechanisms affecting binding and entry of liposome-DNA complexes in poorly differentiated *versus* partially differentiated airway cells that are more representative of airway epithelia *in vivo*.

For these studies, we utilized *in vitro* cell models, which allow us to examine discrete levels of cellular differentiation within the same cultures. Because RTE cells are readily available and the cultures are highly reproducible, the detailed studies were pursued in the RTE system. We also studied cationic liposome transfection of human bronchial epithelial cells and observed very similar patterns of cell growth and transfectability (Fig. 1). Thus, we believe it is likely that similar mechanisms govern susceptibility to cationic liposome-mediated gene transfer in airway epithelial cells of both species.

Morphological studies of day 5 RTE cells show that the central cells of cellular islands exhibit cell-cell interactions (tight junctions and desmosomes) and polarization (perijunctional actin filaments, microvilli, glycocalyx, and a few cilia on the apical surface) (Fig. 2). These morphologic characteristics are much less apparent in the edge cells, consistent with edge cells being less differentiated than central cells. In addition, edge cells extend lamellipodia and filopodia (Fig. 2, *B* and *C*), which are a feature of poorly differentiated regenerating cells (10) and may participate in phagocytic activity. Even at this relatively early stage of redifferentiation, central RTE cells lost their transfectability by liposome-DNA complexes with transgene expression confined primarily to the edge of cellular islands (Fig. 1*B*). We, therefore, examined this stage of RTE cell cultures to determine the cellular mechanisms mediating differences in the transfectability of edge and central cells.

Because cellular proliferation rates have been suggested to be related to transduction efficiency (34, 35), we examined the localization of proliferating cells within the cellular islands. Our results demonstrate that day 5 RTE cells proliferate in a patchy distribution throughout the "islands" (Fig. 3). The different distribution of proliferating cells from transduced cells on the edge indicates that cell proliferation is not the major variable accounting for differential (edge *versus* central) transgene expression in our studies.

Our studies next focused on the differences in liposomal binding and endocytic capacity between edge and central cells of RTE cultures. Fluorescent labeling techniques were used to quantify liposome-DNA complexes *in situ*. LipofectACE® labeled with the lipid dye, CM-DiI, was chosen to detect liposome-DNA complexes, because CM-DiI-labeled LipofectACE® exhibited similar levels of transgene expression as unlabeled LipofectACE® (data not shown). Although unlabeled DOTAP® (Boehringer Mannheim), Lipofectin®, and LipofectAMINE® (Life Technologies) also mediated similar levels of gene transfer efficiency and selective expression in the edge cells, labeling

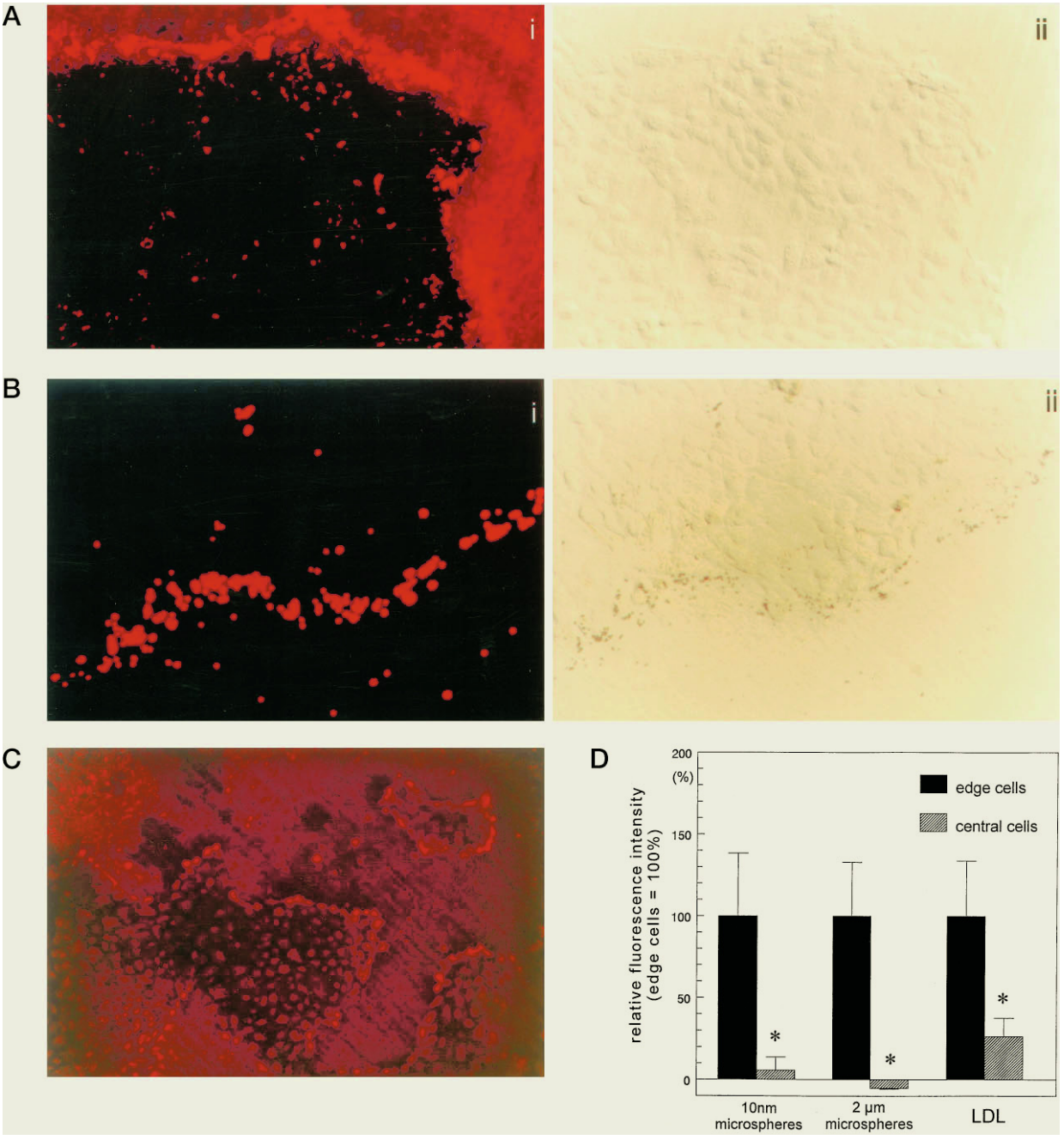

FIG. 7. **Distribution of fluorescently labeled probes of endocytic pathways in day 5 RTE cells at 37 °C.** *A*, 10-nm microspheres (probes of pinocytosis) were taken up preferentially by edge cells, while less signal was detected in the central area. *i*, fluorescent image; *ii*, DIC image. *B*, 2-μm microspheres (probes of phagocytosis) showed a similar pattern to *A*. *i*, fluorescent image; *ii*, DIC image. *C*, most of the cells endocytosed LDL (a probe of receptor-mediated endocytosis), although edge cells internalized more than central cells. *i*, fluorescent image; *ii*, DIC image. *D*, quantification of fluorescence intensity indicated peripheral predominance of internalization of each endocytic marker. Indeed, only LDL was associated with significant central cell internalization (27% that of edge cells). Fluorescence intensity is presented as a percentage relative to the fluorescence intensity of edge cells. Quantitative data are presented as mean ± S.D. ($n = 5$; *, $p < 0.05$).

of these complexes with the fluorescent probes reduced transfection efficiency. Liposome-DNA complexes were labeled with CM-DiI alone when incubated with cells, because the DNA dye, BOBO-1, stained cellular nuclei as well as plasmid DNA and because more than 90% of the labeled liposomes used in our studies were complexed with DNA at the ratio of 1:5 (w/w) (DNA:liposome) (Fig. 4, *A* and *B*).

Almost all edge cells endocytosed liposome-DNA complexes, consistent with selective transgene expression in these cells. In contrast, incubation of labeled liposome-DNA complexes with RTE cells resulted in no uptake of the complexes by central cells (Fig. 5*B*), consistent with the absence of transfection in central cells (Fig. 1). To identify the processes that mediate liposome-DNA complex entry, the binding capacity of RTE cells for liposome-DNA complexes was examined at 4 °C, and surface charge was assessed by cationized ferritin, which attaches to cell surfaces as a function of surface charge (19–21). The binding of liposome-DNA complexes and cationized ferritin occurred selectively on the edge cells (Fig. 5, *A* and *C*, and Fig. 6, *A* and *B*). The negative surface charge may facilitate liposome-DNA complex entry into the edge cells by concentrating and retaining the complexes on the cellular surface such that they are more likely to be endocytosed.

To test whether reduced binding alone is responsible for

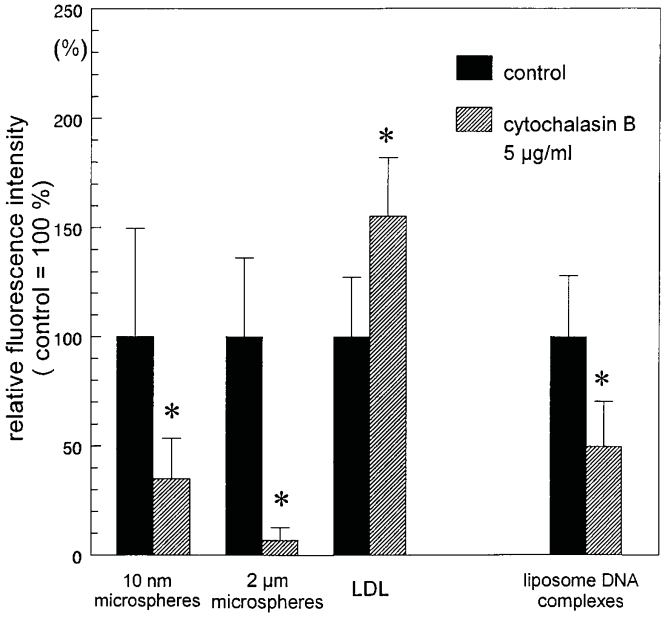

FIG. 8. **Effects of cytochalasin B on endocytosis of liposome-DNA complexes and endocytic markers by edge cells.** Cytochalasin B (5 μg/ml) inhibited pinocytosis of 10-nm microspheres (65%) and phagocytosis of 2-μm microspheres (93%) but not receptor-mediated endocytosis of LDL. Liposome-DNA complex entry was partially (50%) inhibited by cytochalasin B. Fluorescence intensity is presented as a percentage relative to the fluorescence intensity of the controls. Quantitative data are presented as mean ± S.D. ($n = 5$; *, $p < 0.05$).

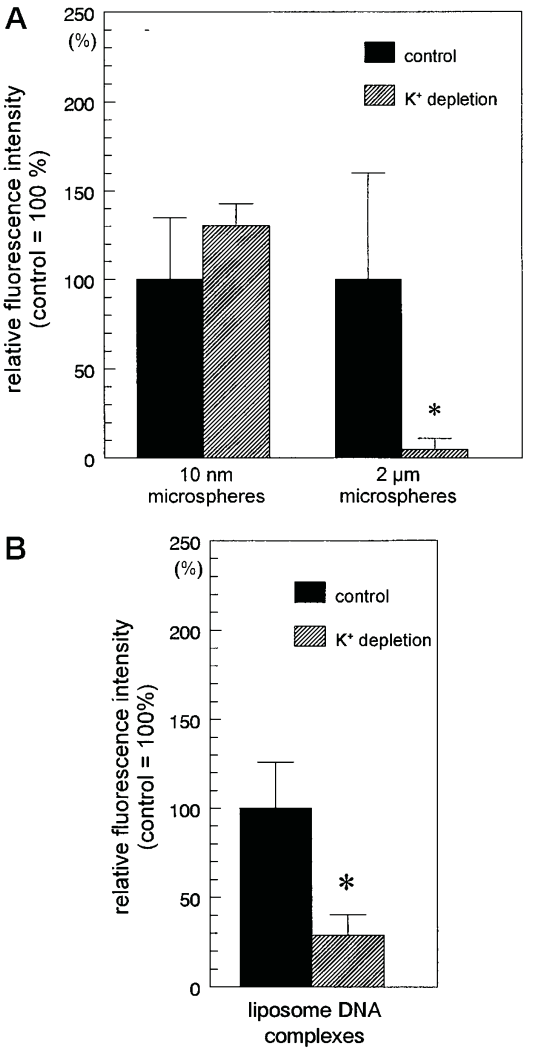

FIG. 9. **Effects of potassium depletion on pinocytosis (10-nm microspheres), phagocytosis (2-μm microspheres), and endocytosis of liposome-DNA complexes by edge cells.** RTE cells were depleted of intracellular potassium and incubated with pinocytic and phagocytic markers and liposome-DNA complexes in potassium-free buffer. *A*, pinocytosis was not affected, but phagocytosis was inhibited with potassium depletion. *B*, liposome-DNA complexes showed decreased entry in potassium-free buffer. Fluorescence intensity is presented as a percentage relative to the fluorescence intensity of the controls. Quantitative data are presented as mean ± S.D. ($n = 5$; *, $p < 0.05$).

reduced cellular entry, we characterized endocytic pathways of both edge and central cells and determined which entry pathway was utilized by poorly differentiated cells to internalize liposome-DNA complexes. Pinocytic and phagocytic activities were examined with 10-nm and 2-μm latex microspheres, respectively, and receptor-mediated endocytosis (endocytosis through coated pits) was detected with DiI-LDL. The edge cells internalized significant quantities of each marker, whereas central cells exhibited receptor-mediated endocytosis but little pinocytic and no phagocytic activity (Fig. 7).

To identify the entry pathway for liposome-DNA complexes in the edge cells, we inhibited pinocytosis and phagocytosis, but not receptor-mediated endocytosis, with cytochalasin B and tested its effects on liposome uptake. Cytochalasin B inhibited entry of 10-nm (65%) and 2-μm (93%) latex microspheres but not entry of LDL (Fig. 8). The same concentration of cytochalasin B decreased endocytosis of liposome-DNA complexes by 50% (when corrected for the binding component, the calculated endocytosis was decreased by 77%), demonstrating that pinocytic or phagocytic mechanisms rather than receptor-mediated endocytosis dominate the internalization process of liposome-DNA complexes.

We utilized intracellular K^+ depletion to distinguish between pinocytosis and phagocytosis as the entry pathway for the liposome-DNA complexes in edge cells. Depletion of K^+ inhibits receptor-mediated endocytosis by removing membrane-associated clathrin coat with no effects on pinocytosis (25). The clathrin coat also appears to be involved in phagocytosis. Aggeler and Werb (28) have reported that half of phagosomes have clathrin coat on their membranes, and Isberg and Tran van Nhieu (29) suggested that anti-clathrin antibodies inhibit integrin-mediated phagocytosis of bacteria. Therefore, we examined the effects of K^+ depletion on pinocytosis and phagocytosis of latex microspheres to test whether K^+ depletion selectively inhibits phagocytosis in RTE cells. Fig. 9*A* shows that K^+ depletion had no effect on pinocytosis of 10-nm microspheres but inhibited phagocytosis of 2-μm microspheres by more than 90%. The entry pathway for liposome-DNA complexes was subsequently examined using this treatment. Fig. 9*B* shows that K^+ depletion inhibited liposome-DNA complex entry by 71%, suggesting that liposome-DNA complexes enter edge cells primarily by phagocytosis.

This result is consistent with the reports of others. For example, the size of liposome-DNA complexes (200–500 nm or larger) (36, 37) would appear to be too large to allow endocytosis through coated vesicles (average diameter is 110 nm). The charge interaction between the liposome-DNA complexes and the cell surface (38) may also resemble the zipper model of phagocytosis. Finally, electron micrographs from two previous studies (11, 39) suggest morphologically that the predominant pathway for liposome-DNA complex entry into undifferentiated cell lines is phagocytosis. Therefore, we conclude that poorly differentiated edge cells exhibit the phagocytic capacity required for internalization of liposome-DNA complexes, whereas the relatively differentiated central cells lack this key entry pathway for lipid-mediated transfection.

Evaluation of our data emphasizes that transgene expression is inefficient even in the edge cells (Fig. 1) compared with the highly efficient liposome-DNA complex entry into this cell type (Fig. 5). Thus, the rate-limiting process for expression after vector entry requires further investigation in edge cells. The poorly differentiated RTE edge cells may exhibit the same rate-limiting factors, *e.g.* nuclear entry, as the cell lines previously investigated by others (11).

In conclusion, the islands of airway epithelial cells exhibit a spectrum of cellular differentiation that affects gene transfer efficiency. The dedifferentiated and transfectable edge cells of RTE cultures endocytose liposome-DNA complexes consequent to their relatively negative surface charge and phagocytic activity. The central, relatively differentiated cells do not internalize liposome-DNA complexes because of reduced negative surface charge and absence of phagocytosis. We have shown that these findings are generalizable to human airway epithelia (Fig. 1) and to a number of lipid formulations, including those used in human clinical trials. Strategies to overcome these entry barriers may require the use of vectors that take advantage of receptor-mediated endocytosis that exists in differentiated cells or fusogenic virosomal approaches that are independent of plasma membrane endocytic capacity.

Acknowledgments—We thank Kim Burns and Dr. Johnny Carson for electron microscopy studies and Drs. C. William Davis, Margaret W. Leigh, and Hong Ye for helpful discussion.

REFERENCES

1. Felgner, P. L., Gadek, T. R., Holm, M., Roman, R., Chan, H. W., Wenz, M., Northrop, J. P., Ringold, G. M., and Danielsen, M. (1987) *Proc. Natl. Acad. Sci. U. S. A.* **84,** 7413–7417
2. Leventis, R., and Silvius, J. R. (1990) *Biochim. Biophys. Acta* **1023,** 124–132
3. Rose, J. K., Buonocore, L., and Whitt, M. A. (1991) *BioTechniques* **10,** 520–525
4. Hawley-Nelson, P., Ciccarone, V., Gebeyehu, G., and Jessee, J. (1993) *Focus* **15,** 73–79
5. Holmen, S. L., Vanbrocklin, M. W., Eversole, R. R., Stapleton, S. R., and Ginsberg, L. C. (1995) *In Vitro Cell. Dev. Biol.* **30,** 347–351
6. Trivedi, R. A., and Dickson, G. (1995) *J. Neurochem.* **64,** 2230–2238
7. Caplen, N. J. Alton, E. W. F. W., Middleton, P. G., Dorin, J. R., Stevenson, B. J., Gao, X., Durham, S. R., Jeffery, P. K., Hodson, M. E., Coutelle, C., Huang, L., Porteous, D. J., Williamson, R., and Geddes, D. M. (1995) *Nature Med.* **1,** 39–46
8. Grubb, B. R., Pickles, R. J., Ye, H., Yankaskas, J. R., Vick, R. N., Engelhardt, J. F., Wilson, J. M., Johnson, L. G., and Boucher, R. C. (1994) *Nature* **371,** 802–806
9. Knowles, M. R., Hohneker, K. W., Zhou, Z., Olsen, J. C., Noah, T. L., Hu, P.-C., Leigh, M. W., Engelhardt, J. F., Edwards, L. J., Jones, K. R., Grossman, M., Wilson, J. M., Johnson, L. G., and Boucher, R. C. (1995) *N. Engl. J. Med.* **333,** 823–831
10. Dupuit, F., Zahm, J. M., Pierrot, D., Brezillon, S., Bonnet, N., Imler, J. L., Pavirani, A., and Puchelle, E. (1995) *Hum. Gene Ther.* **6,** 1185–1193
11. Zabner, J., Fasbender, A. J., Moninger, T., Poellinger, K. A., and Welsh, M. J. (1995) *J. Biol. Chem.* **270,** 18997–19007
12. Kaartinen, L., Nettesheim, P., Adler, K. B., and Randell, S. H. (1993) *In Vitro Cell. Dev. Biol.* **29,** 481–492
13. Gray, T. E., Guzman, K., Davis, C. W., Abdullah, A. H., and Nettesheim P. (1996) *Am. J. Respir. Cell Mol. Biol.* **14,** 104–112
14. Wu, R., Yankaskas, J. R., Cheng, E., Knowles, M. R., and Boucher, R. C. (1985) *Am. Rev. Respir. Dis.* **132,** 311–320
15. Lechner, J. F., and LaVeck, M. A. (1985) *J. Tiss. Cult. Methods* **9,** 43–48
16. Theriot, J. A., Mitchison, T. J., Tilney, L. G., and Portnoy, D. A. (1992) *Nature* **357,** 257–260
17. Claassen, E. (1992) *J. Immunol. Methods* **231,** 231–240
18. Price, J., Turner, D., and Cepok, C. (1987) *Proc. Natl. Acad. Sci. U. S. A.* **84,** 156–160
19. King, C. A., and Preston, T. M. (1977) *FEBS Lett.* **73,** 59–63
20. Soeiro, M. N. C., Silva-Filho, F. C., and Meirelles, M. N. L. (1994) *J. Submicrosc. Cytol. Pathol.* **26,** 121–130
21. Williams, M. C. (1984) *Proc. Natl. Acad. Sci. U. S. A.* **81,** 6054–6058
22. Pratten, M. K., and Lloyd, J. B. (1986) *Biochim. Biophys. Acta* **881,** 307–313
23. Barak, L. S., and Webb, W. W. (1981) *J. Cell Biol.* **90,** 595–604
24. Brown, E. J. (1995) *BioEssays* **17,** 109–117
25. Larkin, J. M., Brown, M. S., Goldstein, J. L., and Anderson, R. G. W. (1983) *Cell* **33,** 273–285
26. Yu, X. Y., Takahashi, N., Croxton, T. L., and Spannhake, E. W. (1994) *Environ. Health Perspect.* **102,** 1068–72
27. Anderson, J. M., and van Itallie, C. M. (1995) *Am. J. Physiol.* **269,** G467–G475
28. Aggeler, J., and Werb, Z. (1982) *J. Cell Biol.* **94,** 613–623
29. Isberg, R. R., and Tran van Nhieu, G. (1995) *Trends Cell Biol.* **5,** 120–124
30. Yoshimura, K., Rosenfeld, M. A., Nakamura, H., Sherer, E. M., Pavirani, A., Lecocq, J. P., and Crystal, R. G. (1991) *Nucleic Acids Res.* **20,** 3323–3340
31. Sorscher, E. J., Logan, J. J., Frizzell, R. A., Lyrene, R. K., Bebok, Z., Dong, J. Y., DuVall, M., Felgner, P. L., Matalon, S., and Walker, L. (1994) *Hum. Gene Ther.* **5,** 1259–1277
32. Hyde, S. C., Gill, D. R., Higgins, C. F., Trezise, A. E. O., MacVinish, L. J., Cuthbert, A. W., Ratcliff, R., Evans, M. J., and College, W. H. (1993) *Nature* **362,** 250–255
33. Logan, J. J., Bebok, Z., Walker, L. C., Peng, S., Felgner, P. L., Siegel, G. P., Frizzell, R. A., Dong, J., Howard, M., Matalon, S., Lindsey, J. R., DuVall, M., and Sorscher, E. J. (1995) *Gene Ther.* **2,** 38–49
34. Nicolau, C., and Sene, C. (1982) *Biochim. Biophys. Acta* **721,** 185–190
35. Takeshita, S., Gal, D., Leclerc, G., Pickering, J. G., Riessen, R., Weir, L., and Isner, J. M. (1994) *J. Clin. Invest.* **93,** 652–661
36. Sternberg, B., Sorgi, F. L., and Huang, L. (1994) *FEBS Lett.* **356,** 361–366
37. Gustafsson, J., Arvidson, G., Karlsson, G., and Almgren, M. (1995) *Biochim. Biophys. Acta* **1235,** 305–312
38. Barthel, F., Remy, J. S., Loeffler, J. P., and Behr, J. P. (1993) *DNA Cell Biol.* **12,** 553–560
39. Zhou, X., and Huang, L. (1994) *Biochem. Biophys. Acta* **1189,** 195–203